LAWRENCE
LIVERMORE
NATIONAL
LABORATORY

LLNL-PROC-656127

Diagnosing residual motion via the x-ray self emission from indirectly driven inertial confinement implosions

A. Pak, J. E. Field, L. R. Benedetti, J. Caggiano, R. Hatarik, N. Izumi, S. F. Khan, J. Knauer, T. Ma, B. K. Spears, R. P. J. Town, D. K. Bradley

June 25, 2014

High Temperature Plasma Diagnostic
Atlanta, GA, United States
June 1, 2014 through June 5, 2014

Disclaimer

This document was prepared as an account of work sponsored by an agency of the United States government. Neither the United States government nor Lawrence Livermore National Security, LLC, nor any of their employees makes any warranty, expressed or implied, or assumes any legal liability or responsibility for the accuracy, completeness, or usefulness of any information, apparatus, product, or process disclosed, or represents that its use would not infringe privately owned rights. Reference herein to any specific commercial product, process, or service by trade name, trademark, manufacturer, or otherwise does not necessarily constitute or imply its endorsement, recommendation, or favoring by the United States government or Lawrence Livermore National Security, LLC. The views and opinions of authors expressed herein do not necessarily state or reflect those of the United States government or Lawrence Livermore National Security, LLC, and shall not be used for advertising or product endorsement purposes.

Diagnosing residual motion via the x-ray self emission from indirectly driven inertial confinement implosions[a)]

A. Pak,[1b)] J. E. Field,[1] L.R. Benedetti,[1] J. Caggiano,[1] R. Hatarik,[1] N. Izumi,[1] S.F. Khan,[1] J. Knauer,[2] T. Ma,[1] B.K. Spears,[1] R.P.J. Town,[1] and D. K. Bradley[1]

[1]*Lawrence Livermore National Laboratory, Livermore, CA, 94550, USA*
[2]*Laboratory for Laser Energetics, Rochester, NY, 14623, USA*

(Presented XXXXX; received XXXXX; accepted XXXXX; published online XXXXX)
(Dates appearing above are provided by the Editorial Office)

In an indirectly driven implosion, non-radial translational motion of the compressed fusion capsule is a signature of residual kinetic energy not coupled into the compressional heating of the target. A reduction in compression reduces the peak pressure and nuclear performance of the implosion. Measuring and reducing the residual motion of the implosion is therefore necessary to improve performance and isolate other effects that degrade performance. Using the gated x-ray diagnostic, the x-ray Bremsstrahlung emission from the compressed capsule is spatially and temporally resolved at x-ray energies of >8.7 keV, allowing for measurements of the residual velocity. Here details of the x-ray velocity measurement and fitting routine will be discussed and measurements will be compared to the velocities inferred from the neutron time of flight detectors.

I. Introduction

At the National Ignition Facility[1], (NIF) indirect drive inertial confinement implosion experiments[2-4] are being conducted with the goal of fusing deuterium and tritium (DT) ions in sufficient quantities such that the resultant neutron and alpha particle yields contain more energy than was used to drive the implosion. In the indirect drive scheme, a laser produced x-ray drive is used to compress a spherical fusion capsule target to sufficient densities and temperatures to initiate a cascade of fusion reactions. Simulations indicate that a low mode asymmetry in radiation flux that drives the implosion, or a low mode asymmetry in the shape of the ideally spherical capsule target, can produce a jet of material that distorts the implosion[5]. This is calculated to reduce the pressure and resulting energy yield of the implosion while the flow of the burning material temporally broadens the detected neutron signal, increasing the apparent temperature. These asymmetries impart residual kinetic energy[6], defined as energy that is not coupled to the radial compression of the target. Low mode drive and capsule asymmetries couple energy into the translational motion of the implosion that can be detected by a suite of neutron time of flight (NTOF) detectors[7-8] as well as by the gated x-ray detector (GXD) diagnostics[9]. Measuring the residual translational velocity of the implosion can help to resolve some of the discrepancy between the measured temperatures and yields and those calculated assuming low mode spherical symmetry of the drive and target. This work details the development of a new technique that that utilizes the observed spatially and temporally resolved x-ray emission to measure the residual velocity imposed on an implosion via a deliberate drive asymmetry.

II. Experiment

As shown in Fig. 1 a), the 192 beams of the NIF laser are used to irradiate the inner wall of a gold cylinder, known as a hohlraum, to create a x-ray drive with a peak temperature of ~300 eV. This x-ray flux ablates the outer plastic surface of the capsule target, thereby driving the implosion. The implosion is driven in this indirect manner to create a spatially smooth x-ray radiation source to minimize the seeding of Rayleigh-Taylor instabilities.

An experiment, denoted here as N130814, was performed to study the effects of drive asymmetries on the implosion performance and to observe clearly the nuclear and diagnostic signatures. In this experiment, an 8% increase and decrease in peak laser power was applied to the lower and upper outer laser cones, respectively. This was calculated to impart a ±2% x-ray drive asymmetry to capsule target and result in a residual velocity of 120 μm/ns in the vertical direction. The symmetry capsule target used had an outer plastic ablator shell, initially 1.138 mm in radius and .209 mm thick, that surrounded a central equimolar DT gas fill, at an initial temperature and density of 32 K and 9.13 mg/cc, respectively. As the implosion compresses the target, the central DT gas was compressed to a radius of ~50 μm and a temperature of ~2.9 keV. The x-ray Bremsstrahlung emission from this so-called 'hot core' is spatially and temporally resolved by the hardened GXD (hGXD) diagnostic. As shown in Fig 1b), this diagnostic uses a pinhole array to image the emission with a spatial resolution of ~10 μm onto a two strip gated micro channel plate (MCP) detector. Each strip has a width of 15 mm and a length of 35 mm and is filtered by 2.5 mm of Kapton. This filtering, in addition to the 2 μm of gold that cover the patch in the hohlraum through which the x-rays are imaged, limits the detected x-rays to energies >8.7 keV. The gain on each strip is temporally gated by a voltage pulse that imparts a gain width ~100 ps in duration. This pulse travels down the length of the strip at a velocity of ~c/2, thereby allowing for a total temporal coverage of ~230 ps per MCP strip. This allows pinhole images created at different locations along the length of the strip to be recorded at different times. Unfortunately, in this experiment, the detector was not optimally timed to observe the peak x-ray emission of the implosion. Here the center of the first strip was timed at -130 ps from peak x-ray emission and the center

[a)]Contributed paper published as part of the Proceedings of the 20th Topical Conference on High-Temperature Plasma Diagnostics, Atlanta, Georgia, June, 2014.
[b)]Author to whom correspondence should be addressed: pak5@llnl.gov

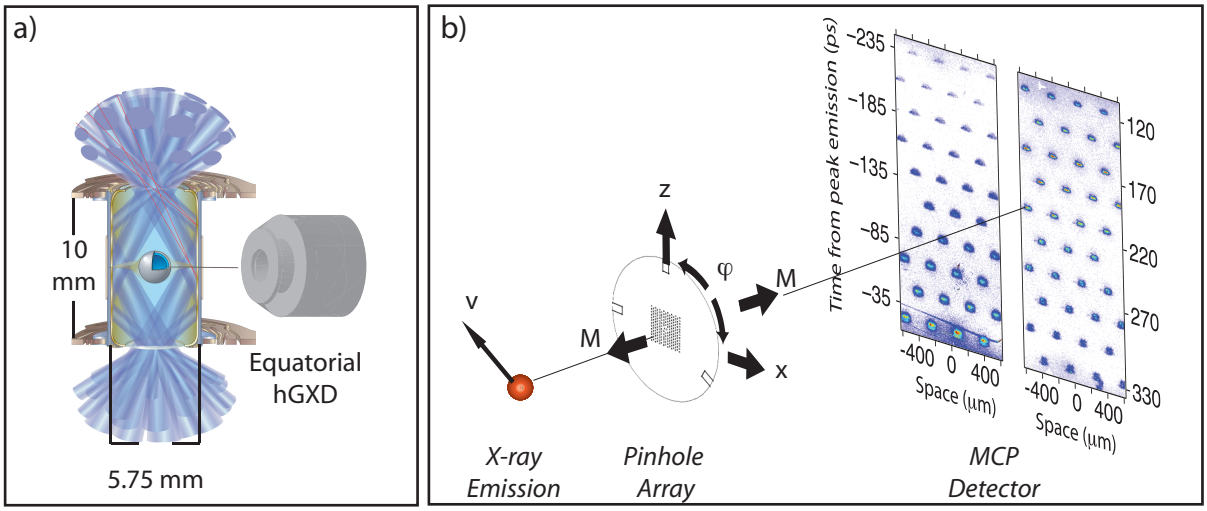

FIG1: (Color online) The indirect drive experimental setup and details of the pinhole imaging performed by the hardened gated x-ray detector diagnostic. a) A gold lined hohlraum, 5.75 mm in diameter and 9.43 mm in length, is irradiated through the upper and lower laser entrance holes by 192 beams of the NIF laser, creating an x-ray drive which implodes the spherical symmetry capsule target placed at the center of the hohlraum. b) The x-ray emission from the implosion is imaged through a hohlraum diagnostic patch along the equatorial axis by a pinhole array onto a gated micro channel plate detector. The 2 μm of gold that cover the diagnostic patch and 2.5 mm of Kapton diagnostic filtering reach a 10% transmission at an x-ray energy of 8.7 keV. The image location is a function of the residual velocity of the implosion as well as the magnification, rotation, and translation imparted by the hardened gated x-ray imaging diagnostic

of the second strip was timed at 220 ps from peak x-ray emission. The velocity, as measured by the NTOF detectors, is expected to reflect the velocity of the implosion over a duration of approximately ±150 ps around peak compression and x-ray emission. Therefore to compare the velocity measured by the x-ray and neutron detectors, only data from the first MCP strip, taken between -140 to -30 ps, was used to fit the x-ray velocity.

III. Method

The residual velocity of the hot spot is found by minimizing the difference between the observed center of x-ray emission and the image emission center that is calculated for a hot spot object given a residual velocity and magnitude of image transformations associated with the magnification, translation and rotation. The x-ray images were analyzed after an 8 μm median blur and background subtraction was applied. Two methods were used to find the center of observed emission, the center of mass and the contour center of emission. These methods were applied after the data below a threshold value was set to zero. As there is uncertainty in the x-ray signal level associated with neutron production, to compare to the NTOF measured velocity, signal thresholds over a range from 50 to 70% of the peak emission were used. An example of this method is shown in Fig. 2.

The location of an x-ray pinhole image on the MCP detector depends on the image magnification of the diagnostic as well as the angular and translational orientation of the pinhole array with respect to the hot spot. Additionally, the image location can be modified by components of the residual hot spot velocity that are in the plane of observation. These degrees of freedom on the image location are shown in Fig. 1 b). For a particular magnitude of each of these transformations, the location of emission in the image plane created by the pinhole array can be written by mathematically the product of homogenous transformation matrices in the following manner.

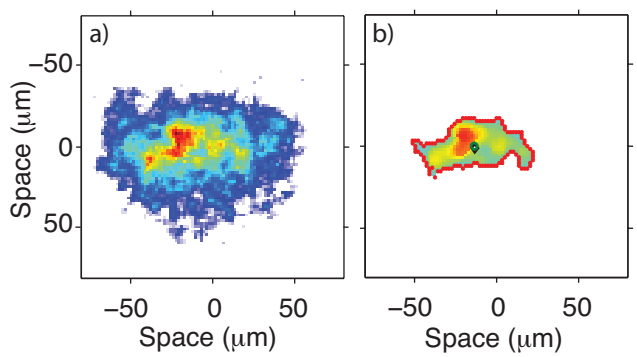

FIG2: (Color online) An example of an x-ray image after background subtraction a), and after a 8 μm median filter and a signal level threshold of 55% of peak value has been applied b). The black diamond and green circle indicate the location o the contour center and centroid, respectively.

$$\overline{I} = \hat{M}(m)\hat{R}(\varphi)\hat{T}(\vec{v}t)\hat{T}(\vec{r})\overline{O} \qquad (1.1)$$

Here, $\overline{O}$ is the location of the emission in the object space, $\hat{T}$, $\hat{R}$, and $\hat{M}$ are the homogenous translation, rotation and magnification transformations, m, φ, $\vec{r}$ and $\vec{v}$ are the magnitude of the magnification, rotation, translation and velocity vectors, t is time and $\overline{I}$ is the projected image location. For each pinhole, a data point homogenous vector $\overline{D}$ is also constructed in the image plane. For each data point, the residual distance between homogenous matrices $\overline{I}$ and $\overline{D}$ is found by applying the inverse translation transformation of vector $\overline{D}$ to $\overline{I}$ (since difference operations are not supported in homogenous notation) and then taking the norm of this quantity. The values of m, φ, $\vec{r}$ and $\vec{v}$

are found by performing a multidimensional minimization of the least squares of the residuals between the observed image and the expected image center yields and can be written as,

$$error = \sum_{i=1}^{n} W_i \left| \hat{T}^{-1}(\overline{D_i})\overline{I_i}(m,\varphi,\vec{v}t,\vec{r}) \right|^2 \qquad \textbf{(1.2)}$$

here $\hat{T}^{-1}$ denotes the inverse translation operation, W_i is an optional weight that can be applied if desired, but was set equal to 1 in this work and n is the number of data points used in the fit. The expected image centers are calculated by applying the aforementioned transformations to the measured pinhole centers obtained from a contact radiograph the of the actual pinhole array used on each experiment. This should remove potential systematic sources of error in pinhole fabrication that would be interpreted as a residual velocity. Additionally the accuracy of the digitization of the recorded film data is expected to be on the order of ±0.16 μm over the 230 ps duration of typical measurements and is expected to impart an uncertainty in the residual velocity of ±1.5 μm/ns.

IV. Results and Discussion

Using the fitting formulism described above, for the applied vertical drive asymmetry on N130814, the x-ray emission from the compressed DT filled symmetry capsule was observed to have an average vertical velocity of 57 ±17 μm/ns and 70 ± 23 μm/ns using the x-ray centroid and contour center locations, respectively. This result compares reasonably well to the measured vertical velocity from the NTOF diagnostics of 74 ± 14 μm/ns. The measured vertical velocities are smaller than the initially predicted residual velocity of 120 μm/ns. The average x-ray velocity was determined by taking the mean velocity over a range of signal thresholds from 50 to 70%. The error bar reported on the average velocity is found by averaging the individual uncertainty over the selected signal thresholds. For each applied signal threshold, the uncertainty in the x-ray velocity measurement was determined by multiplying the average standard deviation in the residual distance between the measure center and the expected center location for groups of pinhole images taken at the same time by the velocity correlation value. The average horizontal velocity of the x-ray emission was found to be -6 ± 17 μm/ns and -21 ± 23 μm/ns whereas the NTOF detectors measured a horizontal velocity of 1 ± 14 μm/ns.

The variation of velocity with contour level could be related to x-ray emission from carbon and silica components of the ablator and capsule gas fill tube material that mix into the hot spot creating locally brighter regions of emission that shift the centroid and contour centers as the signal threshold value is varied. Since this mixed material does not produce neutrons, the NTOFS are not sensitive to this motion. Additionally, for this experiment some discrepancy between the x-ray and neutron inferred velocities could be attributed to fact that the x-ray emission was observed over approximately half the duration of the expected neutron production. Early x-ray images may not be contributing to the production of neutrons and therefore may be weighting the velocity fit incorrectly. Using the same methods, but on an experiment with a so-called hi-foot pulse shape, that has been observed to minimize ablator mix into the hot spot, good agreement in the x-ray velocity across a wide range of contour levels and with the NTOF diagnostics was found and will be discussed in a future publication.

In conclusion, a method of determining the residual translational motion of an indirect drive implosion was developed that utilizes the spatially and temporally resolved x-ray emission from the compressed hot spot. To determine the velocity of the x-ray emission, the observed center of emission over several pinhole images is fit to the projected emission center as calculated by applying image transformations for magnification, rotation, translation and velocity to a initial hot spot object location. For experiment N130814, the observed vertical x-ray velocity was found to be in reasonable agreement with the velocity inferred from the NTOF diagnostics. Future work will incorporate x-ray images from the orthogonal polar line of sight as well as time integrated x-ray images to further describe and constrain the velocity measurement. Discrepancies between observed residual velocities and the velocities predicted from radiation hydrodynamic calculations will be further studied in upcoming experiments with drive asymmetries applied to symmetry capsule and targets with DT fuels layers.

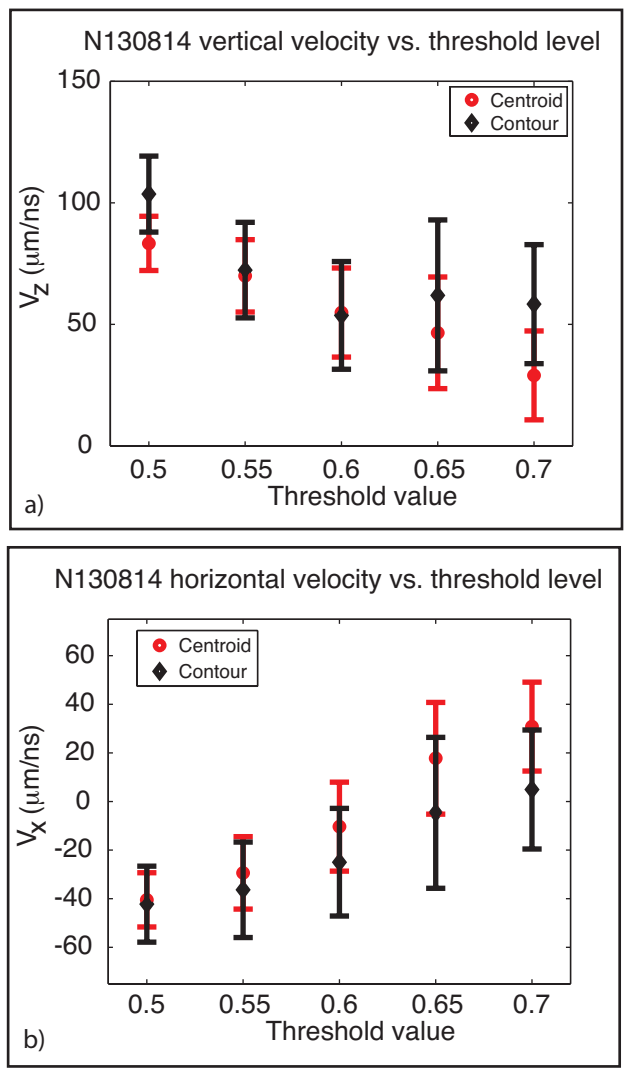

FIG3: (Color online) The results of the velocity fit in the vertical z direction, a) and in the horizontal x direction, b) as a function of signal threshold value for both the contour and centroid method of locating the image center.

This work performed under the auspices of the U.S. Department of Energy by Lawrence Livermore National Laboratory under Contract DE-AC52-07NA27344.

[1] E. I. Moses and C. R. Wuest , Fusion Science. Tech., **71**, 314 (2005).
[2] J. D. Lindl, *et al.*, Phys. Plasmas, **11**, 339 (2004)
[3] S.H Glenzer, *et al.*, Science, **327**, 1228 (2010)
[4] A.J. Mackinnon, *et al.*, Phys. Rev. Lett. **108**, 215005 (2012)
[5] B.K. Spears, *et al.*, Phys. Plasmas, **21**, 042702 (2014)
[6] A. L. Kritcher, *et al.* Phys. Plasmas, **21**, 042708 (2014)
[7] Z.A. Ali, *et al.* Rev. Sci. Instrum., **79** 10E527 (2008)
[8] V.Y. Glebov, *et al.* Rev. Sci. Instrum., **83**, 10D309 (2012)
[9] S. Glenn, *et al.,* Rev. Sci. Instrum. **81**, 10E539 (2010)